RSC Applied Polymers

ROYAL SOCIETY OF CHEMISTRY

PAPER

View Article Online
View Journal | View Issue

Cite this: *RSC Appl. Polym.*, 2024, **2**, 395

Closing the loop: polyimine thermosets from furfural derived bioresources†

Tankut Türel, ‡ Keita Saito,‡ Ivona Glišić, Tim Middelhoek and Željko Tomović *

Over the past few decades, thermosetting plastics have emerged as indispensable materials in both industrial applications and our daily lives, primarily due to their exceptional thermal and mechanical properties resulting from their covalently crosslinked structures. Nevertheless, conventional thermosets face a significant environmental challenge due to their inability to be recycled and reliance on the petroleum resources. Consequently, there is an urgent need to develop innovative, biobased thermosetting materials that are smartly designed to enable efficient chemical recycling, thus contributing to the realization of a circular plastic economy. Here, we present synthesis of a biobased di-furfural monomer and its polymerization with mixtures of various biobased multi-functional amines to construct a library of polyimines. These polyimine thermosets displayed tailor-made thermal and mechanical properties, featuring a wide range of glass transition temperatures from 8 °C to 60 °C and tensile strength spanning from 6.5 to 77.8 MPa. They also demonstrated high char yields, reaching 57% at 800 °C. Notably, these novel polyimines exhibit high bio-content (in the range of 78% to 90%) and closed-loop recyclability under mildly acidic and energy-efficient conditions. This unique property enables the recovery of monomers on demand with high yields and purity. The findings presented in this work represent a valuable contribution in the field of biobased thermosetting polymers with circular economy potential, offering new possibilities for sustainable material design.

Received 2nd December 2023,
Accepted 3rd February 2024

DOI: 10.1039/d3lp00268c

rsc.li/rscapplpolym

Introduction

Over the past few decades, thermosetting plastics have assumed a pivotal role in both industrial applications and our daily lives, thanks to their exceptional thermal and mechanical characteristics stemming from their covalently crosslinked structures.[1] These properties render them indispensable for numerous high-performance sectors, including the automotive and aerospace industries, adhesives, coatings, and composites.[2] However, traditional thermosets suffer from an inherent inability to undergo chemical recycling or reprocessing due to the irreversible nature of their covalent bonds. Consequently, the generated plastic waste is either incinerated or landfilled thereby imposing a substantial environmental burden.[3,4] Furthermore, the prevalent utilization of petroleum-derived monomers in the production of commercial thermosets contributes to increased resource depletion. Therefore, there is a pressing demand to supplant conventional petroleum-based thermosets with biobased alternatives, ideally equipped for closed-loop recycling to recover constituent monomers for reuse in fresh thermoset production. An innovative design of such monomers and their corresponding thermosets holds the promise of achieving circularity, thereby diminishing the carbon footprint of plastics—an outcome of profound significance from both environmental and economic perspectives.[5,6] Incorporation of dynamic and cleavable imine bonds into the designed thermosets has emerged as a prospective solution for monomer recovery and thus achieving circularity as elucidated in prior studies.[7–21]

Previous research endeavors have primarily focused on employing vanillin and its derivatives for the synthesis of biobased polyimine thermosets, aiming to minimize environmental impact.[18–24] For instance, polyimine thermosets, synthesized from a vanillin-based dialdehyde monomer and conventional amine crosslinkers (*i.e.*, diethylenetriamine and tris(2-aminoethyl)amine), displayed tensile strength values ranging from 47 to 57 MPa, accompanied by glass-transition temperatures (T_g) approximately at 60 °C. Remarkably, these thermosets exhibited notable self-healing properties and

Polymer Performance Materials Group, Department of Chemical Engineering and Chemistry, Eindhoven University of Technology, 5600 MB Eindhoven, The Netherlands. E-mail: z.tomovic@tue.nl

†Electronic supplementary information (ESI) available: ^{1}H NMR, ^{13}C NMR and FTIR characterization of the monomer and polyimines; solvent resistivity of the polyimines, thermal and mechanical analysis of the polyimines and the composite. See DOI: https://doi.org/10.1039/d3lp00268c

‡These authors contributed equally.

chemical recyclability in acidic conditions.[14] It was further demonstrated that carbon fibers could be easily retrieved back as pristine quality from the carbon fiber composites of these polyimines through acidic hydrolysis.[24] Another tri-aldehyde-based structure, synthesized from phosphorus oxychloride and vanillin, was employed to produce fire-retardant, recyclable and malleable flexible-to-rigid polyimines, with T_gs and tensile strength ranging between 87 °C to 178 °C and 35.2 to 69.2 MPa, respectively. Particularly, they showed a high limiting oxygen index (LOI) of ~30%.[12] In a separate investigation, the identical tri-vanillin structure was polymerized with Priamine 1071, resulting in a hydrolysable adhesive employed between two iron plates. The adhesive demonstrated a shear strength of 6.79 MPa.[22] Polyimine chemistry extends beyond vanillin derivatives to encompass starch chemistry as well. An illustrative example involves the crosslinking of dialdehyde-modified starch with 1,8-diaminooctane, resulting in a recyclable thermoset characterized by a mechanical strength of 40.6 MPa and a Young's modulus of 1.5 GPa.[15] However, a little attention has been directed toward furfural derivatives in the development of biobased polymers with closed-loop recyclability. 5-Hydroxymethylfurfural (HMF) is a versatile platform chemical that can be converted into a wide range of value-added chemicals.[25] Moreover, HMF and furfural derivatives are typically derived from lignocellulosic biomass,[26,27] and they hold particular significance as the U.S. Department of Energy has classified HMF among the "Top 10" most valuable biomass-derived building blocks.[28] However, HMF is not a stable molecule upon long-term storage. Derivatization is necessary for obtaining more stable monomers (*e.g.*, derivatives such as dialdehyde).[29] For instance, Avérous and colleagues pioneered the development of the first fully biobased, reprocessable polyimine employing 2,5-furandicarboxaldehyde and Priamine 1071, yielding a tensile strength of 0.69 MPa and an elongation at break of 4.4%.[30] Within the same research group, a diverse array of polyimines was designed using the same furan-based dialdehyde in combination with various polyether amines, tailoring mechanical and thermal properties. Notably, the relaxation times and activation energy for dynamic behavior were highly dependent on the crosslink density.[31] In these insightful studies, significant attention has been given to thoroughly investigate thermo-reversibility and vitrimer-like behavior. On the other hand, Kasuya *et al.* developed a library of linear polyimines from bifurfural and rigid to flexible diamines achieving tensile strength ranging from 7.7 MPa to 52.8 MPa; however, they did not focus on either thermal or chemical recycling options.[32] Conversely, imine chemistry provides more than just physical reprocessing; it encompasses chemical recycling as another crucial tool in this context.

Despite numerous prior efforts in furan chemistry, the closed-loop recycling to recover constituent monomers has not yet been demonstrated.[32–36] Moreover, the syntheses of 2,5-furandicarboxaldehyde and bifurfural have proven to be labor-intensive, necessitating costly or heavy metal catalysis, thereby deviating from the principles of green chemistry. 5,5′-[Oxybis (methylene)]bis-2-furfural (OBMF), on the other hand, is a di-furfural containing monomer, which can be prepared in a straightforward manner. Featuring two rigid aromatic units, it stands out as an excellent candidate for the advancement of polyimine thermosets. Therefore, this study aims to reveal a library of closed-loop recyclable polyimines, synthesized from OBMF in conjunction with a mixture of di- and tri-functional amines to establish crosslinked networks (Scheme 1). The resultant polyimine thermosets exhibited tailor-made thermal properties, with T_gs spanning from 8 °C to 60 °C. In addition, these polyimines showed a remarkable char yield, reaching 57% at 800 °C. Furthermore, mechanical testing revealed that these polyimines bestowed elastomeric to rigid thermoset attributes with tensile strength ranging from 6.5 to 77.8 MPa. Of utmost importance, the polyimine thermosets exhibited closed-loop recycling under mildly acidic conditions yielding their constituent monomers. Subsequently, these monomers can be reutilized to yield new thermosets identical to the pristine materials.

Results and discussion

Synthesis and characterization of OBMF monomer

The synthesis of OBMF involves self-etherification of HMF, which requires efficient water removal and acid catalysis (Scheme 1A).[37] Previously, attempts have been made to employ both homogeneous and heterogeneous acid catalysis for this purpose.[38] However, upscale reactions do not result in high yields due to difficulties in removing water from the reaction mixture.[38] This complicates the reaction mixture yielding insoluble humins due to self-polymerization. Consequently, the synthesis was carried out in toluene using a *p*-toluenesulfonic acid catalyst (*p*-TsA) under reflux conditions, employing the Dean–Stark trap.[39] To reduce the formation of self-polymerization products, we hypothesized that dilution could be an effective strategy. Maintaining the concentration of HMF at 0.4 M resulted in an isolated yield of OBMF at 64%. However, reducing the concentration of HMF to 0.1 M significantly improved the isolated yield to 79% (Table S1†). The characterization of OBMF was performed using ^{1}H and ^{13}C NMR in $CDCl_3$ which was supported by FTIR and MALDI-TOF (Fig. S1 and S2†). Accordingly, the aromatic signals were located as two doublets at 7.21 and 6.56 ppm. Two singlets were obtained at 9.62 and 4.63 ppm for the aldehyde and $-CH_2$ protons, respectively. The FTIR gave characteristic carbonyl (C=O) stretching peak for aldehyde at 1670 cm^{-1}, =C–H stretching of the furan ring at 3111 cm^{-1}, aldehydic C–H stretching at 2849 cm^{-1}. Furan ring skeleton vibrations (C=C) were observed at 1524, 1405, 1359 cm^{-1}. In addition, the absorption at 1198 cm^{-1} can be assigned to the inner C–O–C vibration in the furan ring whereas 1040 cm^{-1} shows ether vibration (C–O–C) outside the furan ring.

It's important to highlight that HMF exhibits instability upon storage, owing to the coexistence of reactive aldehyde and alcohol functionalities.[40] During storage, undesired chemical reactions can take place, such as etherification, ester-

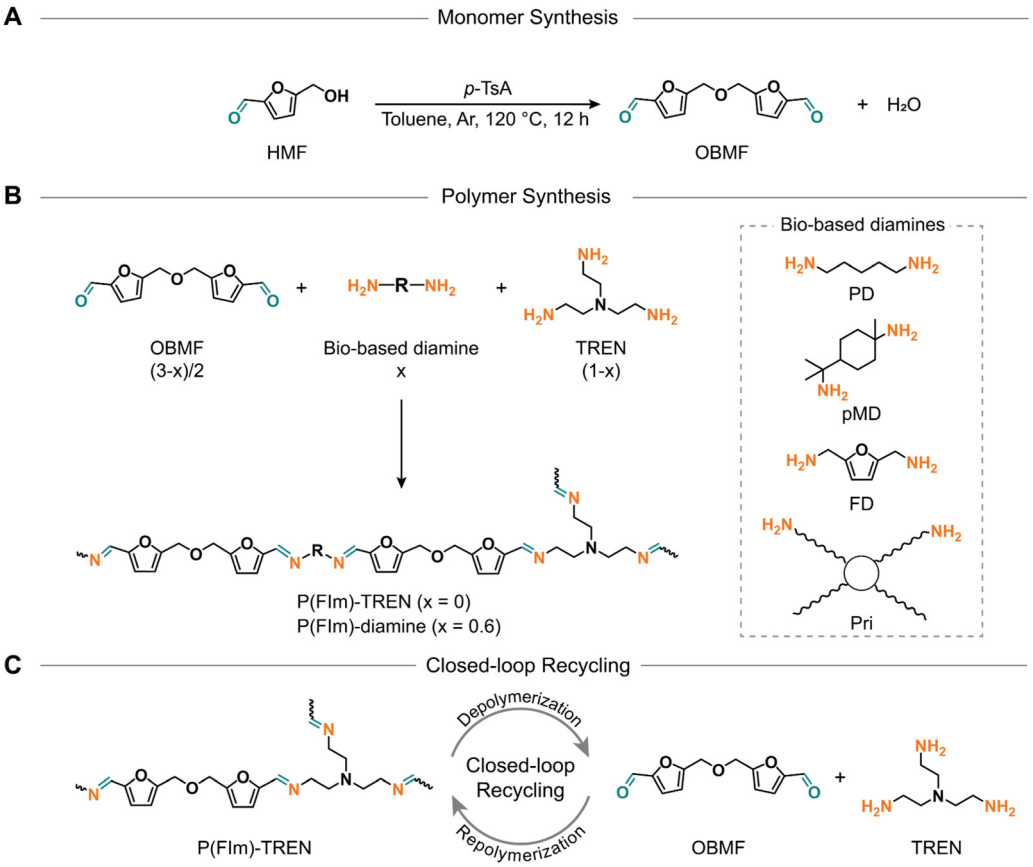

Scheme 1 Synthetic scheme for OBMF (A) and resultant furfural based polyimine networks (B). Schematic illustration of the closed-loop recycling of P(FIm)-TREN (C).

ification, aldol condensation, and acetalization. These reactions lead to the formation of OBMF and insoluble humins.[40] On the contrary, OBMF is highly stable[29] under ambient conditions even after 1 year, as ^{1}H and ^{13}C NMR were identical with the fresh OBMF (Fig. S3†).

Synthesis and structural characterization of polyimine networks

To investigate the relationship between structure and properties, we utilized four biobased diamines (*i.e.*, 1,8-diamino-*p*-menthane (*p*MD), 1,5-diaminopentane (PD), furan-2,5-diyldimethanamine (FD), and Priamine 1071 (Pri))[41] along with tris (2-aminoethyl)amine (TREN) to create a crosslinked polymer network (Scheme 1B). To expand our understanding of these polyimines, we formulated crosslinked polymer networks using flexible or rigid diamines alongside TREN as the crosslinking unit (molar ratio of diamine/TREN = 3/2) as illustrated in Scheme 1B and Table S2.† According to this formulation, the proposed structures have a high bio-content ranging from 78% to 90% by weight (Table 1).

The condensation reactions were conducted in DMF at 80 °C under N_2 environment, and the resulting polymer samples were obtained through solvent casting, polymer drying, and hot-pressing at 120 °C. Structural characterization of the polyimine networks was performed using FT-IR (Fig. S4†). In the FT-IR spectra, a new peak emerged around 1645 cm^{-1}, corresponding to the C=N stretch vibration, while the signal at 1670 cm^{-1}, indicative of the C=O stretch absorption band of aromatic aldehydes, disappeared. Moreover, the networks demonstrated high stability in water and various organic solvents with differing polarities at room temperature for 24 h (Tables S3, 4, Fig. S5 and 6†).

Thermal and mechanical characterization of polyimine networks

The thermal characteristics of the networks were investigated using thermogravimetric analysis (TGA) and differential scanning calorimetry (DSC) under a N_2 atmosphere. In Fig. 1A, the TGA thermograms of the polyimine networks are depicted. All networks exhibited robust thermal stability under N_2, displaying multistep degradation, with their onset degradation temperatures ($T_{d5\%}$) falling between 212 and 306 °C (as shown in Fig. 1A, Table 1 and Fig. S7†). The char residues were significantly high reaching 57%. The substantial residual weights observed in these polyimines indicate the unique characteristics of the furan ring, suggesting a potential formation of graphitic structures upon thermal degradation.[32,42] Moreover, the char residues of P(FIm)-TREN, P(FIm)-PD, P(FIm)-*p*MD and

Table 1 Characteristics of the polyimine networks

	Biobased weight content (%)	$T_{d5\%}$ (°C)	R_{800} (%)	T_g (DSC) (°C)	T_g (DMA) (°C)	E'_{30} (MPa)	E (MPa)	σ_m (MPa)	ε_b (%)
P(FIm)-TREN	78	239	53	54	60	3100	2537 ± 58	70.9 ± 0.9	4.3 ± 0.2
P(FIm)-PD	81	274	57	28	40	1800	896 ± 163	38.7 ± 1.5	9.7 ± 1.6
P(FIm)-*p*MD	83	212	47	51	54	2500	2518 ± 64	69.8 ± 1.1	4.2 ± 0.2
P(FIm)-FD	81	212	57	61	60	3200	2781 ± 73	77.8 ± 1.4	4.5 ± 0.5
P(FIm)-Pri	90	306	26	−15	8	25	16 ± 4	6.5 ± 0.5	37.3 ± 1.9

$T_{d5\%}$: temperature of 5% weight loss. R_{800}: char residue at 800 °C. T_g (DSC) and T_g (DMA): glass transition temperatures obtained from DSC and DMA, respectively. E'_{30}: storage modulus at 30 °C obtained from DMA. E: Young's modulus, σ_m: ultimate tensile strength, ε_b: elongation at break. A trace amount of DMF was found in the final thermosetting polyimines through FTIR analysis (C═O stretching at ~1660 cm^{-1}), potentially contributing to the early weight loss ($T_{d5\%}$) in the materials.

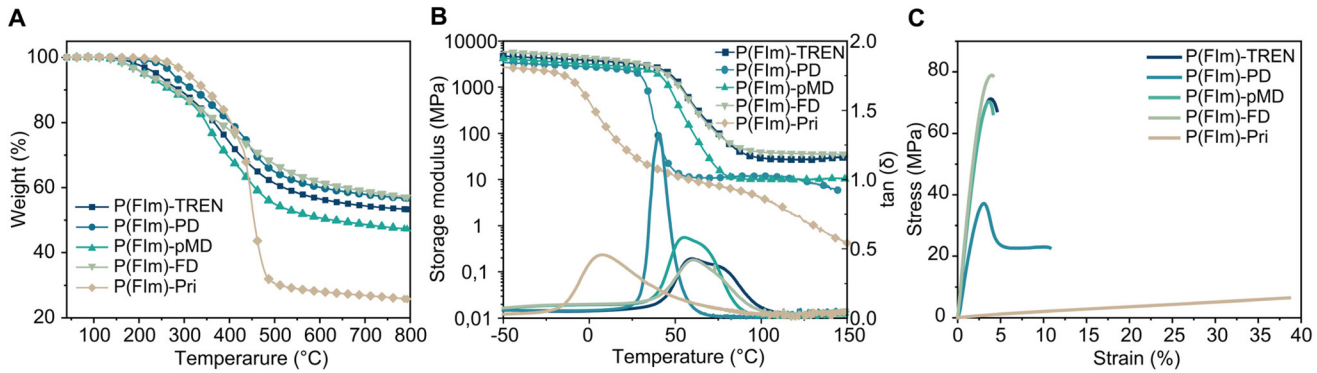

Fig. 1 Characterization of the polyimine networks: TGA (A), DMA (B) and tensile stress–strain tests (C).

P(FIm)-FD were notably higher at 53%, 57%, 47% and 57%, respectively, compared to that of P(FIm)-Pri (26%) at 800 °C. This significant difference is sourced from the higher aromatic segment contents in the former networks.[43,44] The DSC results suggested that the highest T_g was obtained with the most rigid network, P(FIm)-FD, with 61 °C, whereas the fatty diamine containing P(FIm)-Pri gave the lowest T_g of −15 °C (*vide infra*, Table 1 and Fig. S8†).

The thermomechanical characteristics of the networks were assessed using dynamic mechanical analysis (DMA), (Fig. 1B, Table 1 and Fig. S9†). At 30 °C, the storage moduli (E'_{30}) for the P(FIm)-FD, P(FIm)-TREN and P(FIm)-*p*MD networks were 3200, 3100 and 2500 MPa, respectively. In contrast, significantly lower values were observed for the P(FIm)-PD and P(FIm)-Pri networks (1800 MPa for P(FIm)-PD and 25 MPa for P(FIm)-Pri). This discrepancy could be attributed to variations in flexibility, rigidity, and the proportion of aromatic units.[45] As the ratio of aromatic units increased and chain length of the diamines decreased, the material's stiffness escalated, resulting in a larger storage modulus. Moreover, the maxima of the tan δ *versus* temperature plots were identified as the T_g of the networks (Fig. 1B and Table 1). The T_g values obtained from DMA aligned with the trends observed in the results from DSC. Accordingly, the highest T_g of 60 °C was obtained with the most rigid networks P(FIm)-FD and P(FIm)-TREN, which was followed by P(FIm)-*p*MD with T_g of 54 °C. More flexible network P(FIm)-PD gave slightly lower T_g of 40 °C, whereas that of the fatty alkyl chain containing P(FIm)-Pri network was significantly lower at 8 °C due to its highest flexibility.

The mechanical assessment of the networks was performed through tensile tests (Table 1 and Fig. 1C). Across the new networks, the tensile strength ranged from 6.5 to 77.8 MPa, accompanied by 4–37% elongation. Notably, the P(FIm)-FD network exhibited the superior Young's modulus of 2781 MPa, attributed to its highest content of rigid aromatic units. Following closely were P(FIm)-TREN and the cycloaliphatic diamine-containing P(FIm)-*p*MD networks, both showcasing nearly identical Young's moduli of 2537 and 2518 MPa, respectively, owing to their structurally rigid architectures. Given that these three networks displayed nearly identical elongation-at-break values at 4.2–4.5%, the tensile strength of P(FIm)-FD stood out as the highest at 77.8 MPa. In comparison, P(FIm)-TREN and P(FIm)-*p*MD demonstrated slightly lower tensile strengths of 70.9 and 69.8 MPa, respectively. When the rigid cycloaliphatic diamine was replaced with flexible linear aliphatic diamine (*i.e.*, P(FIm)-PD), the mechanical properties were influenced drastically with tensile strength of 38.7 MPa and elongation at break of 9.7%. Conversely, the fatty alkyl chain containing P(FIm)-Pri displayed a tensile strength of 6.5 MPa and an elongation at break of 37.3%. Furthermore, the Young moduli of the flexible networks P(FIm)-PD and P(FIm)-Pri were 896 and 16 MPa, respectively. These observations distinctly indicated that employing an aro-

matic or cycloaliphatic amine resulted in stiffer networks, aligning well with the trend observed in storage modulus. In addition, evidently, employing shorter chains or increasing the content of the rigid segments positively influenced the Young modulus and tensile strength values with decreased elongation at break due to reduced flexibility.[46]

We additionally fabricated a 2-ply carbon fiber reinforced composite utilizing the P(FIm)-TREN network to obtain CFRP (FIm)-TREN (Table S2†). This resulting composite exhibited a Young's modulus of 10.7 GPa and a tensile strength of 295.1 MPa (refer to Fig. S10†). To gain a more comprehensive insight into the interface between the carbon fiber and the network, we conducted SEM analysis to the fractured fibers. The SEM image illustrated that the fibers were thoroughly coated with the polyimine network (Fig. S11†), suggesting a good interaction between the network and carbon fibers which could be through π–π stacking.

Closed-loop recycling through chemical depolymerization

As imine bonds can be conveniently cleaved under acidic conditions,[47,48] we subjected P(FIm)-TREN to a solution of MeTHF and 1 M HCl (v : v = 2 : 8) at 50 °C for 24 hours with continuous stirring (Scheme 1C). Within several hours, the bulk material started to break. The formed OBMF crashed out as a fine powder while TREN·HCl remained dissolved in the aqueous mixture. Upon completion of the depolymerization, OBMF was filtered out and aqueous phase was further extracted with ethyl acetate to get rid of the remaining small amount of OBMF. Collected OBMF fractions were combined, washed with isopropanol and dried in a vacuum oven at 60 °C, achieving a recovery yield of 97%. Furthermore, TREN was recovered in 55% yield from the acidic supernate by neutralizing the HCl salt using a basic anion-exchange resin (Amberlyst A26) and subsequent solvent removal. The high purity and chemical integrity of the recovered monomers were confirmed by ^{1}H NMR spectroscopy (Fig. 2A and B), establishing their suitability for generating fresh thermosets and thereby closing the recycling loop. The recovered monomers were then reused to fabricate recycled rP(FIm)-TREN. Fig. 3 shows that the pristine P(FIm)-TREN and recycled rP(FIm)-TREN have almost the identical properties (Fig. S12†).

Recovering carbon fiber from composites holds significant importance due to the high cost and energy-intensive nature of carbon fiber production.[49] Recycling offers the opportunity to repurpose these premium-quality fibers, allowing for their reuse in various applications. The carbon fiber recovery from the traditional thermosets is a tedious process in which the quality of fibers are lost significantly.[50] In this context, the carbon fiber reinforced polyimine composite was exposed to 1 M HCl at 50 °C for 24 h. Such a mild recovery method plays a crucial role in maintaining the original structure of the virgin carbon fibers as well as the constituent monomers. As evident

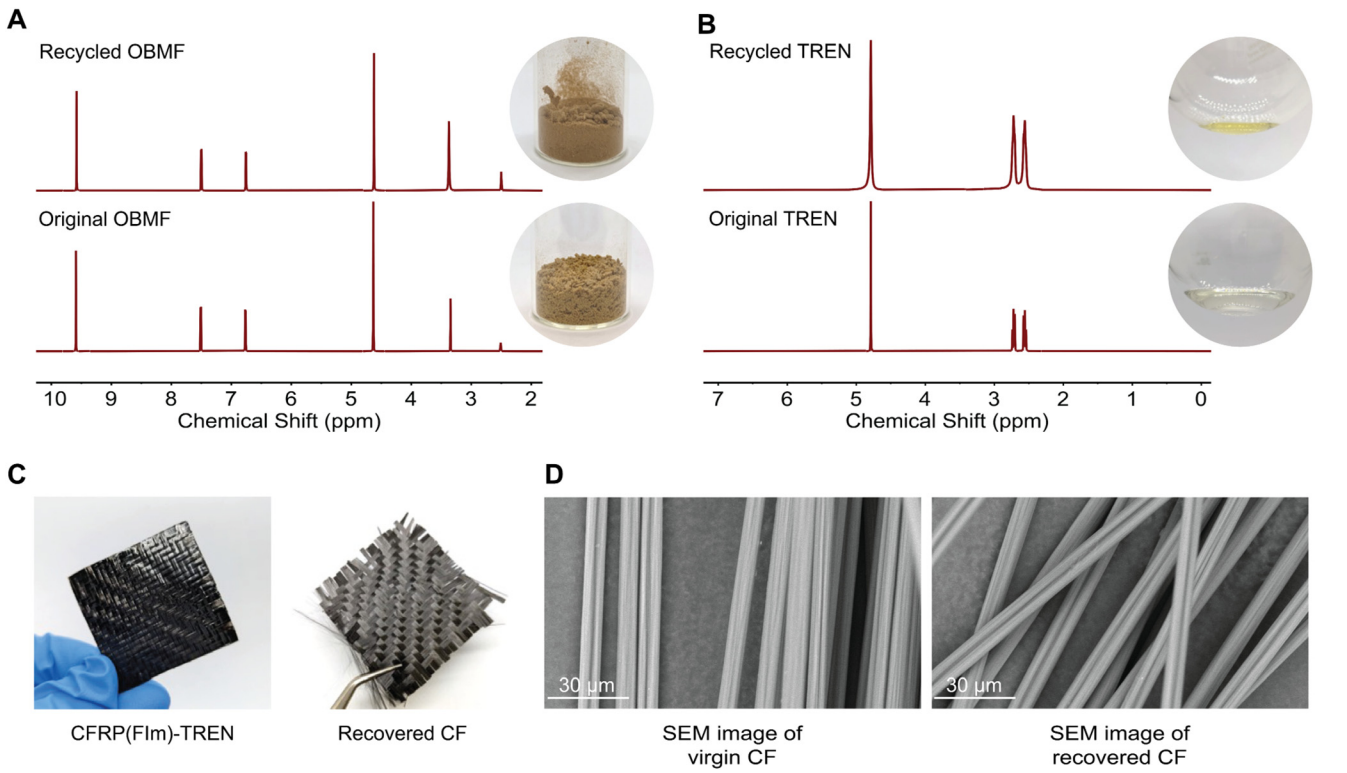

Fig. 2 Chemical recycling of P(FIm)-TREN: physical appearance and ^{1}H NMR spectra of OBMF in DMSO-d_6 (A) and TREN in D_2O (B) after depolymerization and subsequent purification, visual appearance of CFRP(FIm-TREN) and recovered carbon fiber cloth upon depolymerization of the composite (C), SEM images of virgin and recovered carbon fibers (D). Scale bar is 30 μm.

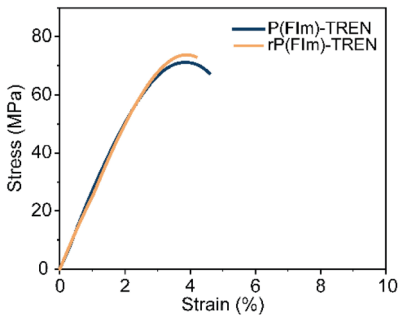

Fig. 3 Stress–strain curves of pristine polyimine P(FIm)-TREN and chemically recycled polyimine rP(FIm)-TREN.

from the SEM images (Fig. 2D), the fibers exhibited pristine quality after undergoing acidic treatment. This proof-of-concept study shows that these chemistry can be applied for chemical recycling of polymer composites.

Conclusions

In this study, we successfully developed a range of biobased, closed-loop recyclable, high-performance polyimines derived from biobased OBMF monomer. These polyimines exhibited a spectrum of properties spanning from elastomeric to rigid behavior, with their glass transition temperature window falling between 8 to 60 °C and tensile strength ranging from 6.5 to 77.8 MPa. Notably, a carbon fiber reinforced composite crafted from these polyimines demonstrated a high tensile strength of 295.1 MPa. Moreover, despite their exceptional resistance to organic solvents and water, these polyimines can undergo in a closed-loop recycling scheme under mildly acidic conditions. This process facilitates the retrieval of constituent monomers in high yield and purity, along with the recovery of carbon fibers having pristine quality. We believe this research is a step forward in developing eco-friendly thermosetting polymers sourced from bio-derived monomers. It opens up exciting opportunities for creating sustainable materials in a way that promotes a circular economy.

Experimental

Materials

Tris(2-aminoethyl)amine (96%, TREN), *para*-toluenesulfonic acid monohydrate (*p*-TsA, 98.5%), 1,8-diamino-*p*-menthane (85%, *p*MD) and Amberlyst A26 hydroxide form were procured from Merck. 5-Hydroxymethylfurfural (98%, HMF) was obtained from Manchester Organics. 1,5-Diaminopentane (98%, PD) was sourced from ABCr GmbH, while furan-2,5-diyldimethanamine (95%, FD) was purchased from BLD Pharmaceuticals. Priamine 1071 was obtained from Croda. Toluene, chloroform, isopropanol, ethyl acetate, and dimethylformamide (DMF) were obtained from Biosolve B.V. 2-Methyltetrahydrofuran (MeTHF) was purchased from TCI. $CDCl_3$ (99.9% D) and DMSO-d_6 (99.9% D) were purchased from Cambridge Isotope Laboratories whereas D_2O (99.9% D) was ordered from Merck. Carbon fibers (S-CF-22-21-Pro) were sourced from EasyComposites.

Methods

The ^{1}H NMR and ^{13}C NMR spectra were acquired using a Bruker UltraShield (400 MHz) with $CDCl_3$, DMSO-d_6 or D_2O as the solvent. Mass spectrometry analysis employed a Bruker Autoflex III TOF/TOF MALDI analyzer. FTIR spectra were recorded using a Thermo Scientific Nicolet iS20 FTIR spectrometer averaging eight scans across the wavenumber range of 450–4000 cm^{-1}.

Swelling measurements and gel fraction tests were performed in several organic solvents (*i.e.*, methanol, ethanol, acetone, IPA, THF, hexane) and water. Swelling ratios were calculated using the eqn (1), where q represents the swelling ratio, W_0 the initial weight of the network, W_s the weight of swollen network.[51,52]

$$q = 100 \times \frac{W_s - W_0}{W_0} \quad (1)$$

Gel fractions were calculated using eqn (2), where φ stands for gel fraction, W_0 is the initial weight of the polymer, and W_1 the weight after drying.[51,52]

$$\phi = 100 \times \frac{W_1}{W_0} \quad (2)$$

Thermogravimetric analyses (TGAs) were conducted utilizing a TA Instruments TGA550, heating 5–10 mg samples from 100 to 800 °C under an N_2 atmosphere. DSC measurements were carried out with a TA Instruments Q2000, where samples (5–15 mg) were placed in an Aluminum-Hermetic pan. The experiments ran from −50 to 180 °C at a rate of either 10 °C min^{-1} or 20 °C min^{-1} under an N_2 atmosphere. Glass transition temperatures (T_g) were determined by identifying the midpoint of the reversible endotherm during the second heating.

Dynamic Mechanical Analysis (DMA) measurements were conducted using TA Instruments DMA850. The experiments were carried out from −80 °C to 150 °C at a heating rate of 3 °C min^{-1} under an oscillatory strain of 0.1% and a frequency of 1 Hz with a preload force of 0.05 N. The glass transition temperature (T_g) was identified as the peak value of tan δ.

The tensile tests were performed with a Zwick/Roell Intelligent testing with 1 kN load cell using dumbbell-shaped specimens (effective length: 12 mm, width: 2 mm, and measured thickness around 0.6 mm) at a strain rate of 50 mm min^{-1} and a pre-load of 0.1 N (exceptionally, the strain rate for the composite was 10 mm min^{-1}). The Young modulus of the materials was determined by calculating the slope of the derivative of the stress–strain curves from 0.1 to 1% strain. To determine the experimental error, a set of five samples was employed.

Scanning electron microscopy (SEM, Phenom ProX) was used to investigate the surface of the carbon fibers at an acceleration voltage of 15 kV.

Synthesis of OBMF

HMF (12.6 g, 99.9 mmol) was dissolved in 750 ml of toluene in a three-necked round bottom flask equipped with a Dean–Stark trap. After purging for 10 minutes with Ar, *p*-TsA (250 mg, 1.3 mmol) was added. The temperature of the reaction mixture was then raised to 120 °C and the mixture was kept stirring at this temperature under Ar flow for 12 hours. Upon completion of the reaction, toluene was evaporated, leaving black solids. These solids were sonicated in chloroform (200 ml) and the mixture was filtered through a silica plug. Silica plug was further washed with ethyl acetate (100 ml) to ensure there is no OBMF stuck. The collected filtrate was evaporated, and the obtained solids washed with isopropanol (100 ml) and filtered to obtain a light brown powder. Finally, the product was dried in a vacuum oven at 60 °C to yield light brown powder (9.1 g, 79%).

^{1}H NMR (400 MHz, $CDCl_3$) δ 9.62 (s, 2H), 7.21 (d, J = 3.5 Hz, 2H), 6.56 (d, J = 3.5, 2H), 4.63 (s, 4H). ^{13}C NMR (101 MHz, $CDCl_3$) δ 177.86, 157.34, 152.92, 121.99, 111.99, 64.75. MS (MALDI-TOF) m/z: $[M + Na^+]^+$ calculated for $C_{12}H_{10}NaO_5^+$ 257.04, found 257.04.

Preparation of the polyimine networks

OBMF, TREN, and various diamines were individually dissolved in DMF (refer to Table S2†) at a monomer concentration of 0.1 g ml^{-1}. These mixtures were poured into a PTFE tray, dried in a nitrogen oven at 80 °C for 24 hours, followed by additional drying in a vacuum oven at the same temperature for another 24 hours. The precured P(FIm)s were then subjected to hot pressing at 120 °C for 30 minutes (at 0 kN for 10 minutes, followed by 50 kN for the subsequent 20 minutes) to produce polyimine films.

Preparation of the carbon-fiber reinforced polyimine network: CFRP(FIm)-TREN

OBMF and TREN were individually dissolved in DMF (refer to Table S2†) at a monomer concentration of 0.1 g ml^{-1}. These mixtures were poured into a PTFE tray, containing 2-ply carbon fiber cloth, dried in a nitrogen oven at 80 °C for 24 hours, followed by additional drying in a vacuum oven at the same temperature for another 24 hours. The precured P(FIm)-TREN was then subjected to hot pressing at 120 °C for 30 minutes (at 0 kN for 10 minutes, followed by 50 kN for the subsequent 20 minutes) to produce carbon-fiber reinforced polyimine film.

Chemical recycling of P(FIm)-TREN and carbon fibers repolymerization

5 grams of P(FIm)-TREN was dispersed in a solution of MeTHF : HCl (2 : 8 by volume, 100 ml). The mixture was stirred at 50 °C for 24 hours. Once depolymerization was completed, OBMF was filtered, and the aqueous phase was extracted further with EA to eliminate any remaining traces of OBMF. The collected OBMF fractions were combined, rinsed with isopropanol, and dried in a vacuum oven at 60 °C, achieving a recovery yield of 97%. Additionally, TREN was obtained with a yield of 55% from the acidic supernatant by neutralizing the HCl salt using an alkaline anion-exchange resin, Amberlyst A26, and subsequent solvent evaporation. The same reaction condition was applied to CFRP(FIm)-TREN. At the final stage, the carbon fibers were further washed with ethyl acetate and water to remove any soluble traces of monomers.

Upon separation of the monomers, recycled polyimine network rP(FIm)-TREN was prepared in the same way as the pristine one.

Conflicts of interest

There are no conflicts to declare.

Acknowledgements

The authors gratefully acknowledge Mr Chang-lin Wang for experimental support (Scanning Electron Microscopy).

References

1 S. Ma and D. C. Webster, *Prog. Polym. Sci.*, 2018, **76**, 65–110, DOI: 10.1016/j.progpolymsci.2017.07.008.
2 M. Gilbert, Brydson's Plastics Materials, Amsterdam, 2017. ISBN: 978-0-323-35824-8.
3 F. Gamardella, S. De la Flor, X. Ramis and À. Serra, *Polym. Eng.*, 2022, 1–46, DOI: 10.1515/9783110733822-001.
4 T. Türel, Ö. Dağlar, F. Eisenreich and Ž. Tomović, *Chem. – Asian J.*, 2023, **18**, e202300373, DOI: 10.1002/asia.202300373.
5 C. Jehanno, M. M. Pérez-Madrigal, J. Demarteau, H. Sardón and A. P. Dove, *Polym. Chem.*, 2019, **10**, 172–186, DOI: 10.1039/C8PY01284A.
6 L. T. J. Korley, T. H. Epps, B. A. Helms and A. J. Ryan, *Science*, 2021, **373**, 66–69, DOI: 10.1126/science.abg4503.
7 W. Denissen, J. M. Winne and F. E. Du Prez, *Chem. Sci.*, 2016, **7**, 30–38, DOI: 10.1039/C5SC02223A.
8 P. Taynton, K. Yu, R. K. Shoemaker, Y. Jin, H. J. Qi and W. Zhang, *Adv. Mater.*, 2014, **26**, 3938–3942, DOI: 10.1002/adma.201400317.
9 C. J. Kloxin and C. N. Bowman, *Chem. Soc. Rev.*, 2013, **42**, 7161–7173, DOI: 10.1039/C3CS60046G.
10 G. M. Scheutz, J. J. Lessard, M. B. Sims and B. S. Sumerlin, *J. Am. Chem. Soc.*, 2019, **141**, 16181–16196, DOI: 10.1021/jacs.9b07922.
11 P. Taynton, H. Ni, C. Zhu, K. Yu, S. Loob, Y. Jin, H. J. Qi and W. Zhang, *Adv. Mater.*, 2016, **28**, 2904–2909, DOI: 10.1002/adma.201505245.
12 S. Wang, S. Ma, Q. Li, W. Yuan, B. Wang and J. Zhu, *Macromolecules*, 2018, **51**, 8001–8012, DOI: 10.1021/acs.macromol.8b01601.
13 S. Kim, A. Rahman, M. Arifuzzaman, D. Gilmer, B. Li, J. K. Wilt, E. Lara-Curzio and T. Saito, *Sci. Adv.*, 2022, **8**, eabn6006, DOI: 10.1126/sciadv.abn6006.

14 H. Geng, Y. Wang, Q. Yu, S. Gu, Y. Zhou, W. Xu, X. Zhang and D. Ye, *ACS Sustainable Chem. Eng.*, 2018, **6**, 15463–15470, DOI: **10.1021/acssuschemeng.8b03925**.
15 H. Zhang, Z. Su and X. Wang, *ACS Sustainable Chem. Eng.*, 2022, **10**, 8650–8657, DOI: **10.1021/acssuschemeng.2c02537**.
16 P. Yu, H. Wang, T. Li, G. Wang, Z. Jia, X. Dong, Y. Xu, Q. Ma, D. Zhang, H. Ding and B. Yu, *Adv. Sci.*, 2023, **10**, 2300958, DOI: **10.1002/advs.202300958**.
17 K. Fukuda, M. Shimoda, M. Sukegawa, T. Nobori and J. Lehn, *Green Chem.*, 2012, **14**, 2907, DOI: **10.1039/c2gc35875a**.
18 K. Saito, F. Eisenreich, T. Türel and Ž. Tomović, *Angew. Chem., Int. Ed.*, 2022, **61**, e202211806, DOI: **10.1002/anie.202211806**.
19 K. Saito, T. Türel, F. Eisenreich and Ž. Tomović, *ChemSusChem*, 2023, **16**, e202301017, DOI: **10.1002/cssc.202301017**.
20 T. Türel and Ž. Tomović, *ACS Sustainable Chem. Eng.*, 2023, **11**, 8308–8316, DOI: **10.1021/acssuschemeng.3c00761**.
21 C. L. Wang, F. Eisenreich and Ž. Tomović, *Adv. Mater.*, 2023, **35**, 2209003, DOI: **10.1002/adma.202209003**.
22 Z. Zhou, X. Su, J. Liu and R. Liu, *ACS Appl. Polym. Mater.*, 2020, **2**, 5716–5725, DOI: **10.1021/acsapm.0c01008**.
23 K. A. Stewart, J. J. Lessard, A. Cantor, J. F. Rynk, L. M. Bailey and B. S. Sumerlin, *RSC Appl Polym*, 2023, **1**, 10–18, DOI: **10.1039/D3LP00019B**.
24 Y. Wang, A. Xu, L. Zhang, Z. Chen, R. Qin, Y. Liu, X. Jiang, D. Ye and Z. Liu, *Macromol. Mater. Eng.*, 2022, **307**, 2100893, DOI: **10.1002/mame.202100893**.
25 R. Van Putten, J. C. Van Der Waal, E. De Jong, C. B. Rasrendra, H. J. Heeres and J. G. De Vries, *Chem. Rev.*, 2013, **113**, 1499–1597, DOI: **10.1021/cr300182k**.
26 X. Zhang, S. Xu, Q. Li, G. Zhou and H. Xia, *RSC Adv.*, 2021, **11**, 27042–27058, DOI: **10.1039/D1RA04633K**.
27 A. Jaswal, P. P. Singh and T. Mondal, *Green Chem.*, 2022, **24**, 510–551, DOI: **10.1039/D1GC03278J**.
28 J. J. Bozell and G. R. Petersen, *Green Chem.*, 2010, **12**, 539–554, DOI: **10.1039/B922014C**.
29 B. F. M. Kuster, *Starke*, 1990, **42**, 314–321, DOI: **10.1002/star.19900420808**.
30 S. Dhers, G. Vantomme and L. Avérous, *Green Chem.*, 2019, **21**, 1596–1601, DOI: **10.1039/C9GC00540D**.
31 R. Hajj, A. Duval, S. Dhers and L. Avérous, *Macromolecules*, 2020, **53**, 3796–3805, DOI: **10.1021/acs.macromol.0c00453**.
32 Y. Tachibana, S. Hayashi and K.-I. Kasuya, *ACS Omega*, 2018, **3**, 5336–5345, DOI: **10.1021/acsomega.8b00466**.
33 H. Nabipour, H. Niu, X. Wang, S. Batool and Y. Hu, *React. Funct. Polym.*, 2021, **168**, 105034, DOI: **10.1016/j.reactfunctpolym.2021.105034**.
34 Y. Jing, Z. Xu, Y. Wu, M. Jiang, Z. C. Zhang and G. Zhou, *ACS Sustainable Chem. Eng.*, 2022, **10**, 4404–4414, DOI: **10.1021/acssuschemeng.1c07038**.
35 Y. Jiang, J. Yun and X. Pan, *ACS Sustainable Chem. Eng.*, 2022, **10**, 16555–16562, DOI: **10.1021/acssuschemeng.2c04141**.
36 M. Fache, C. Montérémal, B. Boutevin and S. Caillol, *Eur. Polym. J.*, 2015, **73**, 344–362, DOI: **10.1016/j.eurpolymj.2015.10.032**.
37 W. Fan, C. Verrier, Y. Queneau and F. Popowycz, *Curr. Org. Synth.*, 2019, **16**, 583–614, DOI: **10.2174/1570179416666190412164738**.
38 M. Annatelli, G. Trapasso, D. D. Torre, L. Pietrobon, D. Redolfi-Bristol and F. Aricò, *Adv. Sustainable Syst.*, 2022, **6**, 2200297, DOI: **10.1002/adsu.202200297**.
39 D. Chundury and H. H. Szmant, *Ind. Eng. Chem. Prod. Res. Dev.*, 1981, **20**, 158–163, DOI: **10.1021/i300001a022**.
40 H. Shen, H. Shan and L. Liu, *ChemSusChem*, 2020, **13**, 513–519, DOI: **10.1002/cssc.201902799**.
41 V. Froidevaux, C. Négrell, S. Caillol, J. Pascault and B. Boutevin, *Chem. Rev.*, 2016, **116**, 14181–14224, DOI: **10.1021/acs.chemrev.6b00486**.
42 N. Amini, K. Aguey-Zinsou and Z. Guo, *Carbon*, 2011, **49**, 3857–3864, DOI: **10.1016/j.carbon.2011.05.022**.
43 Z. Xu, Y. Liang, X. Ma, S. Chen, C. Yu, Y. Wang, D. Zhang and M. Miao, *Nat. Sustainable*, 2020, **3**, 29–34, DOI: **10.1038/s41893-019-0444-6**.
44 R. Jeng, S.-M. Shau, J. Lin, W. Su and Y. Chiu, *Eur. Polym. J.*, 2002, **38**, 683–693, DOI: **10.1016/S0014-3057(01)00246-4**.
45 X. Liu, E. Zhang, Z. Feng, J. Liu, B. Chen and L. Liang, *J. Mater. Sci.*, 2021, **56**, 15733–15751, DOI: **10.1007/s10853-021-06291-5**.
46 X. Xu, S. Ma, J. Wu, J. Yang, B. Wang, S. Wang, Q. Li, J. Feng, S. You and J. Zhu, *J. Mater. Chem. A*, 2019, **7**, 15420–15431, DOI: **10.1039/C9TA05293C**.
47 P. Wu, X. Wang, R. Shi, H. Cheng and F. Zhao, *Green Chem.*, 2022, **24**, 1561–1569, DOI: **10.1039/D1GC04441A**.
48 M. E. Belowich and J. F. Stoddart, *Chem. Soc. Rev.*, 2012, **41**, 2003–2024, DOI: **10.1039/C2CS15305J**.
49 T. Liu, J. Peng, J. Liu, X. Hao, C. Guo, R. Ou, Z. Liu and Q. Wang, *Composites, Part B*, 2021, **224**, 109188, DOI: **10.1016/j.compositesb.2021.109188**.
50 B. Wang, S. Ma, S. Yan and J. Zhu, *Green Chem.*, 2019, **21**, 5781–5796, DOI: **10.1039/C9GC01760G**.
51 H. Zhang, D. Wang, W. Liu, P. Li, J. Liu, C. Liu, J. Zhang and N. Zhao, *J. Polym. Sci., Part A: Polym. Chem.*, 2017, **55**, 2011–2018, DOI: **10.1002/pola.28577**.
52 T. Türel, B. Eling, A. M. Cristadoro, T. Mathieu, M. Linnenbrink and Ž. Tomović, *ACS Appl. Mater. Interfaces*, 2024, **16**, 6414–6423, DOI: **10.1021/acsami.3c17416**.